

Intelligent Production Modeling Using Full Field Pattern Recognition

Y. Khazaeni, SPE, and S.D. Mohaghegh, SPE, West Virginia University

Summary

Production-data analysis has been applied extensively to predicting future production performance and field recovery. These applications operate mostly on a single-well basis. This paper presents a new approach to production-data analysis using artificial-intelligence (AI) techniques in which production history is used to build a fieldwide performance-prediction model. In this work, AI and data-driven modeling are used to predict future production of both synthetic- (for validation purposes) and real-field cases.

In the approach presented in this article, production history is paired with field geological information to build data sets containing the spatio-temporal dependencies among different wells. These dependencies are addressed by compiling information from closest offset wells (COWs) that includes their geological and reservoir characteristics (spatial data) as well as their production history (temporal data).

Once the data set is assembled, a series of neural networks are trained using a back-propagation algorithm. These networks are then fused together to form the intelligent time-successive production-modeling (ITSPM) system. This technique uses only the widely available measured data such as well logs and production history of existing wells to predict future performance of the existing wells and production performance of the new (infill) wells. To demonstrate the applicability of this method, a synthetic oil reservoir is modeled using a commercial simulator. Production and well-log data are extracted into an all-inclusive data set. Several neural networks are trained and validated to predict different stages of the production. The ITSPM method is used to estimate the production profile for nine new wells in the reservoir. Furthermore, ITSPM is also applied to two giant oil fields in the Middle East. The first one has more than 200 wells and 40 years of production history. ITSPM's production predictions of the four newest wells in this reservoir are compared with their actual production. The second real field has hundreds of wells producing from multiple layers. The field has undergone waterflooding for almost its whole life. This case also shows the capabilities of this technique in more-complex scenarios and especially multiphase systems.

Introduction

Two of the most influential pieces of information in decision making and field developments are our depth of knowledge about the reservoir's state of depletion and the estimation of the remaining reserves. These become more important in brownfields where most wells are in their decline period and new wells can easily become unprofitable if not drilled in the right spots.

Reservoir engineers use numerical models and try to adjust their performance to match the observed behavior in the field. This process is called history matching, and it involves building a numerical model that can mimic the available historical data. This ability can ensure that the reservoir model is capable of forecasting the future behavior of the field (Fanchi 2005). These models normally are based on numerical solutions of the fluid-flow equation and require fairly accurate data and measurements of the formation. Furthermore, acquiring such data and measurements is expensive, and building full-field models to use these data in

a cohesive manner can be financially prohibitive considering the computational and human resources required.

In contrast, instead of lengthy and expensive numerical solutions, analytical solutions are simpler and less costly. These solutions are normally limited to single-well-based analyses with many limiting homogeneity assumptions. Although these solutions are much easier to develop and they do not need vast amounts of data or of computer power, they are limited in applicability.

Relying on availability of large amounts of data and measurements about the field is not always a realistic solution. Therefore, numerical solutions are not always practical. Moreover, single-well-analysis techniques are not always good choices for field-development strategy and decision making.

Brownfields with marginal production rates or old fields without state-of-the-art technology studies are not the best candidates for costly numerical-simulation models. In some cases, single-well numerical models are built for some fields; these models limit the analysis to one well and do not give a full-field understanding of the reservoir. When numerical models are out of the picture, traditionally empirical models such as decline curves and type curves are used (Arps 1945; Fetkovich 1980). These methods have been updated and improved since their inception (Carter 1981; Agarwal et al. 1999). However, most of these methods are focused at a single-well level and they do not provide a full-field model. More discussion on these methods is provided in the next section. In contrast to the traditional production-data-analysis methods, data-driven models have been introduced and studied in recent years (Mohaghegh et al. 2005; Mohaghegh 2009; Gomez et al. 2009). One of the advantages of these methods is their ability to perform the analysis with a limited amount of data (Mohaghegh 2009; Gomez et al. 2009). On the other hand, using high-level methods of AI, the new methods can move from the single-well prospect to a full-field image of the reservoir. This advantage enables the reservoir engineer to perform full-field analysis for a field that has only production-rate data and possibly some well logs.

ITSPM is a technique that uses production-rate data from existing wells in the field along with any available well logs in order to build a fieldwide production prediction model. Information from multiple wells is fused together and a spatio-temporal database is generated for the entire field. Neural networks are used to infer a coherent model that is able to predict the existing and future well-production behavior.

By using geostatistics methods such as ordinary kriging, the field properties obtained from well logs are mapped throughout the reservoir. This brings out the spatial dependencies throughout the reservoir and tries to employ them in predicting the future of the reservoir. The geostatistics application in this level of modeling also leads to a higher-resolution reserves estimation from the field compared with techniques that do not employ geostatistics. However, this method of reserves estimation cannot predict any heterogeneities that are beyond what the ordinary kriging method can capture.

Production-Data-Analysis Background

Mature fields that have been producing for a long time do not provide much reservoir-characterization data. This is because of their age and the lack of historical data from their old wells. In the time that oil price might not be in its highest range, infill-drilling decisions should be made with a better degree of understanding from such fields in order to have an economically better decision.

Using production data as a tool in decision making has been an interest of petroleum engineers for many years. Different methods

have been developed in this area (Arps 1945). The main limitations that come with production-data-analysis methods relate to the subjectivity of the process. Also, as mentioned previously, most of these analyses are based on single-well studies, failing to provide a full-field, cohesive model that can be used for production-prediction purposes (Mohaghegh et al. 2005). Systematic production-data analysis begins in the techniques presented by Arps (1945). This method is called decline-curve analysis and is still being used as an empirical method. The decline-curve method is very simple and tries to predict the production behavior by fitting an exponential curve to the production history, thereby not requiring any reservoir or well parameters. Arps' decline equation is

where $b = 0$ and $b = 1$ are the exponential and harmonic decline, respectively. Any value of b between 0 and 1 represents a hyperbolic decline. Even though the Arps equation is designed for pseudosteady-state conditions, it has been misused often for oil and gas wells in their transient state.

Following the work of Arps, Fetkovich (1980) paired that with the transient-analytical solutions and generated a set of type curves for oil wells producing at a constant pressure. The Arps and Fetkovich methods both can calculate the well's ultimate recovery under same production setting.

The Carter (1981) gas-system type curves are an extension of Fetkovich type curves for gas wells. A variable λ is used to identify the magnitude of the pressure drawdown in gas wells, where $\lambda = 1$ corresponds to $b = 0$ in Fetkovich liquid-decline curves and characterizes a liquid system curve with an exponential decline. Curves with $\lambda = 0.5$ and 0.75 are for gas wells with an increasing magnitude of pressure drawdown.

Agarwal et al. (1999) introduced a method for production-data analysis. This technique combines decline-curve and type-curve concepts for estimating reserves and other reservoir parameters for oil and gas wells using production data.

Another method was introduced by Palacio and Blasingame (1993), which provides information on gas in place, permeability, and skin.

All methods described here focus on the analysis for one well. No spatial or temporal information from other wells is used in order to enhance the production prediction for that well. This will make these methods fall short in terms of identifying any dependency between different wells in a field.

Methodology

This section introduces a step-by-step procedure for ITSPM. The first step, which is a vital point to this method, is data preparation. In any data-driven technique, preparing the data is very critical, and the success of the project depends on how this step is performed. Having enough data and compiling a comprehensive data set that provides a complete representation of the system's behavior will determine the success of the analysis. Methods that are based on data analysis cannot predict anything above and beyond the data being used for their development. Nevertheless, AI technology allows the extraction of maximum information (in the form of pattern recognition) from the data, information that may not be readily extractable by using conventional techniques.

ITSPM uses well-log data and production history to build an inclusive data set for the entire field. This data set has a record for each well at each timestep of its life. The static information of the reservoir such as rock and fluid characteristics at the well location are included in this record. Furthermore, previous and current production for that well and its neighbors are included. Each record represents a point in time and space. Correlations between these data points can be revealed by means of pattern-recognition techniques. This information is used to build a predictive model that can predict the well's future using the past of the well itself and of the offset well.

In any field, spatial dependencies are a function of the degree of heterogeneity of the reservoir. The more heterogeneous the

reservoir is, the more influential our knowledge of the spatial characteristics will be. The heterogeneity in the reservoir characteristics is addressed by using a geostatistical estimation method throughout the reservoir. The geostatistical method (ordinary kriging) provides a spatial distribution for each parameter rather than assuming a unique value for each parameter around the well. These distributions give a better understanding of the spatial changes for each parameter compared with the homogeneous model. However, the real heterogeneity of the reservoir can be captured only with more sampling of the field.

Spatio-temporal dependencies of flow characteristics of different wells are modeled in a systematically integrated and cohesive manner. The distance between wells and offsets can act as a measure of spatial dependency between wells' behavior. Also, the age difference between wells and their offset wells is a measure of the influence each of the offset wells can have on the wells' production performance.

Modeling is performed using neural networks as universal function approximators. The related training and verification processes are also explained in much more detail later in this manuscript. Upon completion of training, these models are incorporated into a fully automatic prediction system (ITSPM). This tool will use the trained networks to predict the field's production behavior for an extended time period. In this way, a fieldwide comprehension of the reservoir is generated on the basis of a single well's performance history.

A simplified flow chart of the ITSPM method is illustrated in Fig. 1.

Field Description

A commercial numerical-simulation package was used to build a heterogeneous single-layer, single-phase (oil) reservoir. The structure map and well locations are obtained from data related to a real reservoir. Other properties such as porosity, permeability, and initial-water-saturation maps are generated synthetically. A Cartesian-grid system with an average grid size of 200×500 ft and 10,000 gridblocks is used in the numerical-simulation model (**Fig. 2**).

All the reservoir-characteristic ranges are shown in **Table 1**. The distribution for porosity, permeability, and pay thickness is also shown in **Fig. 3**.

Production starts in January 1982 and continues for 15 years. For 55 months, 165 wells are drilled, or three wells per month. Initial pressure is equal to 4,000 psi. All wells are producing on a constant bottomhole pressure equal to 1,500 psi, and bubblepoint pressure is equal to 1,000 psi. Therefore, all the wells are producing oil and solution gas. No free gas exists in the reservoir.

Single-Well Models and Fieldwide Integrations

The objective in this step is to generate single-well models that can be integrated into a fieldwide comprehension of the reservoir. The first step is to define a boundary for each well. This is made possible by using the theory of image wells and the creation of no-flow boundaries between two wells. This theory implies that if two wells start producing at the same time at a distance of R with the same production rate, assuming a homogeneous formation, a no-flow boundary will be created at the same distance to both wells.

Voronoi Delineation. The theory of image wells can be implemented by using the Voronoi graph theory. Having two or more but a finite number of distinct points in the Euclidean plane, all locations in that space can be associated with the closest member of the point set with Euclidean distance being the metric. The result is a tessellation of the plane into a set of the polygons associated with members of the point set. This is called the planar ordinary Voronoi diagram generated by the point set, and the regions constituting the Voronoi diagram are called ordinary Voronoi cells (Okabe et al. 2000).

Using the well locations as generating points, a Voronoi diagram is generated for the entire field. This is done with a sweeping technique over all the gridblocks. For each gridblock, the Euclidean distance from that block to all the wells is calculated. Each

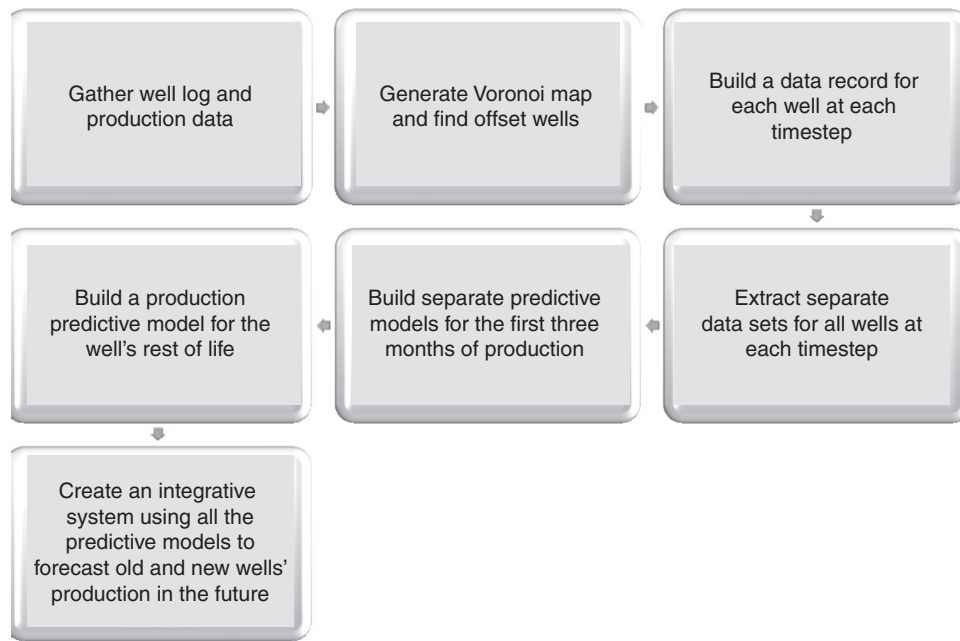


Fig. 1—Intelligent time-successive production-modeling flow chart.

block would belong to the Voronoi cell of the well that it is closest to. That well will be called the “parent well” for that gridblock. By sweeping all the blocks with this method, the entire reservoir is delineated into different Voronoi cells each one of which creates its own parent well’s estimated ultimate drainage area (EUDA).

This process is illustrated in **Fig. 4**. In this work, the ordinary Voronoi diagram is used, meaning no heterogeneity of the reservoir is incorporated in generating the Voronoi diagram. However, by incorporating the knowledge of heterogeneity of reservoir characteristics into the Euclidian distance calculation, the assumption of homogeneity can be removed.

These Voronoi cells are dynamic throughout the life of the reservoir, meaning that if a new well is drilled the ultimate drainage areas for other wells shrink in a way that accommodates the new well. This will continue as long as new wells are being drilled. Using these Voronoi cells, we can account for the reservoir characteristics around the wells by averaging these parameters throughout each cell. Combining the information from closest offset wells and the dynamic value of EUDA at each time with the wells’ static and dynamic information, one coherent database is built for the entire reservoir.

Data Assimilation

The production data alone have a vast amount of information about the reservoir that has been infused to one value of production rate.

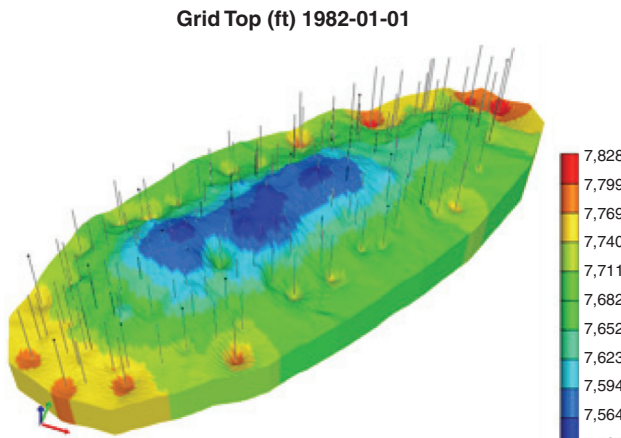


Fig. 2—Schematic of the synthetic reservoir.

Once these data are commingled with the available static and dynamic information of the reservoir, a cohesive full-field model can be generated that represents the reservoir in a predictive way.

Two different kinds of dependencies exist between the production data and reservoir characteristics: (1) the spatial dependencies that are defined by the dependency of production rate on different properties in different locations of the reservoir and (2) the temporal dependencies, defining the dependency of each well’s performance on the history of its own production and that of other wells. In this work, we have tried to address these two issues with one predictive system. In order to do this, we must construct a comprehensive data set on the basis of the reservoir characteristics and the production history.

Thinking clearly about the dependencies between behaviors of all the wells in a field, the closer the wells are the more correlated their behavior would be.

Using this fact in order to introduce the spatial and temporal dependencies, we find the five COWs for each well and include their static and dynamic information in that well’s data record (**Fig. 5**).

Production rate is recorded monthly therefore, at each month a new data record for each well is produced that includes both the static information that does not change over time and the dynamic production data. Moreover, the COWs’ static information and their production data are also included in the data record. Parameters such as distance between the well and offsets and the time difference between their production starting times are also included. This information reflects the significance of dependency between the production behavior of the offsets and that of the well.

Once the data set is generated long enough, it is used to train a neural network that then learns to predict the production rate at next timestep (month).

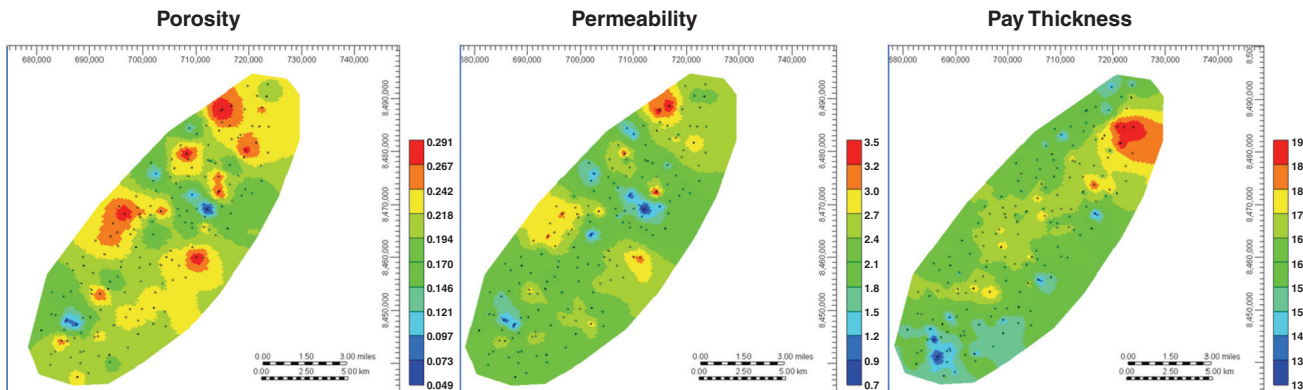
Neural Network Modeling

Artificial neural networks are the naturally inspired part of the AI techniques. They have been used in petroleum engineering since the early 1990s (Mohaghegh 2000) and have shown promising results, especially when it comes to real-time data-driven modeling.

In this study, multilayer neural networks or multilayer perceptrons, are used (Haykin 1999). These networks are most suitable for pattern recognition, especially in nonlinear problems. Networks have one hidden layer with a different number of hidden neurons that are selected on the basis of the number of data records available and the number of input parameters selected in each training process. The training process of the neural networks is conducted

TABLE 1—RESERVOIR-PROPERTY RANGES FOR THE SYNTHETIC RESERVOIR

Property	Porosity	Net Thickness (ft)	Permeability (md)	Initial Water Saturation	Formation Top (ft)
Minimum	0.05	134.04	0.66	0.08	7537.19
Maximum	0.29	192.14	3.54	0.54	7819.38

**Fig. 3—Porosity (fraction), permeability (md), and pay-thickness (ft) distribution in the synthetic reservoir.**

using a back-propagation (Chauvin and Rumelhart 1995) technique. In the training process, the data set is partitioned into three separate segments. This is done in order to make sure that the neural network will not get trapped in the memorization phase (Maren et al. 1990). The partitioning process allows the network to adapt to new data once it is being trained. The first segment, which is the largest of the three, is used to train the network. In order to prevent the memorizing and overtraining effect in the neural-network-training process, a second segment of the data is taken for calibration. This part of the data is not introduced to the network for training, but at each step of the training process, the network is tested for this set. If the updated network gives better predictions for the calibration set, it will replace the previous network; otherwise, the previous network is selected. Training will continue once the error of predictions for both the calibration and the training data set is satisfactory. This will be achieved only if the calibration and training partitions are showing similar statistical characteristics. The third segment of the data set is the verification partition. This part is kept out of the training and calibration process and is used only to test the precision of the network. Once a network is trained and calibrated, the final model is applied to the verification set. If the results are satisfactory, the network is accepted as part of the entire prediction system.

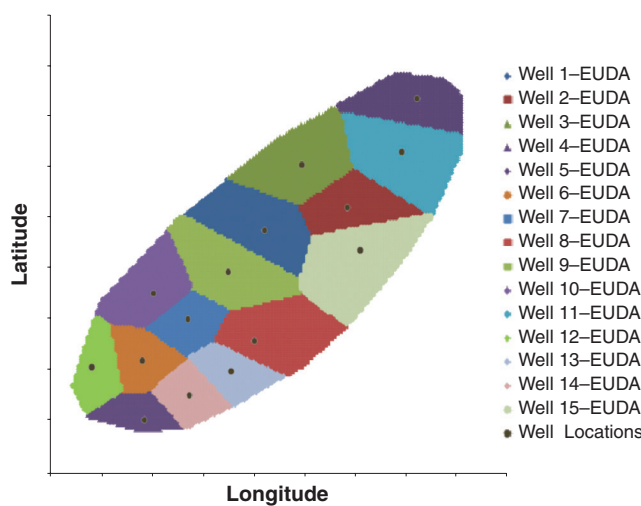
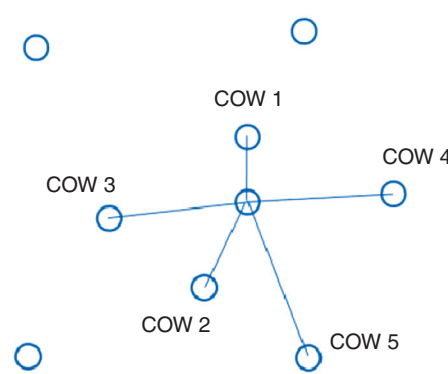
Production Modeling and Prediction

Initial-Rate-Prediction Model. The first step of production prediction is the initial-production-rate estimation. Once each new well is drilled and put into operation, it shows an initial rate of production. This initial production rate depends on the characteristics of the reservoir at that location and also on the production history of the wells surrounding it. The production history represents the degree of depletion of the reservoir at that location. Integrating production rates and reservoir characteristics would lead to a better understanding of the future production behavior.

In a mature field in which wells have been producing for a long time and the reservoir has been depleted at most locations, a new well's initial production rate depends not only on the location's characteristics but also on a function of the well's production starting time; the later the well is drilled, the lower the initial rate may be.

During the reservoir life span, at each time that a new well is drilled, the entire well's information can be a new instance of these dependencies. In order to use this information and infuse it into a predictive model, each well's initial rate and characteristics, along with the dynamic and static information from its offset wells, is recorded just after drilling is completed. This data assimilation leads to a data set that is used to train our first neural-network model (initial-rate-prediction model).

This model, which is trained, calibrated, and verified to predict the initial-production rate of new wells, is designed using a data set built on the basis of the production history of the numerical reservoir model.

**Fig. 4—Voronoi delineation of the synthetic reservoir with 15 wells.****Fig. 5—Five COWs.**

Input Data					
Well's		Closest Offset Wells'			
Static Information	Porosity	Static Information	Porosity	Porosity	
	Formation Thickness		Formation Thickness	Formation Thickness	
	Initial Water Saturation		Initial Water Saturation	Initial Water Saturation	
	Formation Top		Formation Top	Formation Top	
	Location's Lat and Long				
Dynamic Information	Estimated Ultimate Drainage Area	Dynamic Information	Estimated Ultimate Drainage Area	Estimated Ultimate Drainage Area	
	Initial Production Rate				
		Relative Information	Time Difference in Date of first Production	Time Difference in Date of first Production	
			Distance to the Well	Distance to the Well	

Fig. 6—Input-data list for initial-rate-prediction model.

The first 156 wells out of a total number of 165 wells during a 5-year period are used for creating the data set. A total of 156 data records are built, each representing one well at its initial production time. A complete list of inputs that are included in the data set is shown in Fig. 6.

A key-performance-indicator process is performed to rank the most influential input parameters in the initial-production-rate-prediction model. This process takes into account the influence of each input parameter on the output and also the influence of a combination of different input parameters. The top-nine influential parameters are shown in Fig. 7, and the tornado chart shows a comparison of their influence.

Production-Profile-Prediction Model. After estimating the initial production rate for a new well, the production rate is modeled in a time-successive fashion. In other words, at each timestep, the

production rate is predicted on the basis of previous production rates and offset-well information.

In order to increase the accuracy of the prediction at each time, we decided to use the production rate for the past 3 months as input values for the neural network. This can be applied for production modeling through the fourth month. Different models should be created to predict the second and third month of production.

Second- and Third-Month Models. In the second and third months of production, we do not have the advantage of using the last 3 months of production rates as input values because the well has not been producing for 3 months. In this case, two specific neural networks are trained, calibrated, and verified to predict the second and third month of production. In these two networks, respectively, the previous 1 month of production and previous 2 months are used as input values. Input parameters for the second- and third-month production models are presented in Fig. 8.

Input Parameter	% Degree of
Well's Porosity	100
Initial Oil Rate at Offset #1	45
Porosity at Offset #1	39
Oil Rate at Offset #1	32
Initial Oil Rate at Offset #2	30
X Location of the Well	24
Reservoir thickness at the Well	20
Y Location of the Well	19
Oil Rate at Offset #2	18

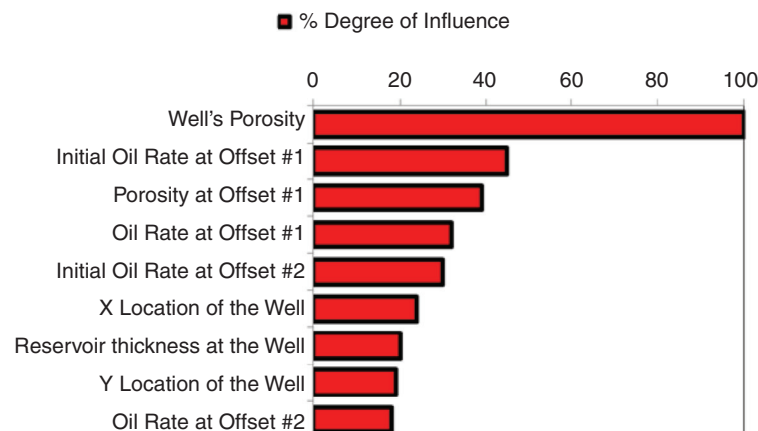


Fig. 7—Top nine influential input parameters.

Input Data						
Well's		Closest Offset Wells'				
Static Information	Porosity	Static Information	Porosity	Porosity		
	Formation Thickness		Formation Thickness	Formation Thickness		
	Initial Water Saturation		Initial Water Saturation	Initial Water Saturation		
	Formation Top		Formation Top	Formation Top		
	Location's Lat and Long					
Dynamic Information	Estimated Ultimate Drainage Area	Dynamic Information	Estimated Ultimate Drainage Area	Estimated Ultimate Drainage Area		
	Initial Production Rate		Initial Production Rate	Initial Production Rate		
			Current Production Rate	Current Production Rate		
		Relative Information	Time Difference in Date of first Production	Time Difference in Date of first Production		
			Distance to the Well	Distance to the Well		

Fig. 8—Input list for second-month (left) and third-month (right) rate-prediction model.

Input Data				
Well's		Closest Offset Wells'		
Static Information	Porosity	Static Information	Porosity	
	Formation Thickness		Formation Thickness	
	Initial Water Saturation		Initial Water Saturation	
	Formation Top		Formation Top	
	Location's Lat and Long	Dynamic Information	Estimated Ultimate Drainage Area	
Dynamic Information	Initial Production Rate		Initial Production Rate	
	Production at 3 months ago		Current Production Rate	
	Production at 2 months ago		Time Difference in Date of first Production	
	Production at 1 month ago		Distance to the Well	

Fig. 9—Input list for tail of production prediction model.

Fourth-Month and After-Production Model (Tail-of-Production Model). Once we have predicted the three initial timesteps, an inclusive neural network is trained for modeling every step of the production profile on the basis of the last three months of production and COW's real-time information.

A list of available inputs for this model is presented in Fig. 9.

One significant difference between this model and the previous three models is the definition of the output parameter. All previous models use production rate as the output. However, to attain more-robust and -accurate results in the fourth model, the output parameter is defined to be the change in production rate from that of the preceding month. This selection has a considerable effect on the final result of production-profile prediction. Had the production rate been selected as the output, sometimes because small changes of rate occur in the tail of production, an increase in the rate would have been observed in the models' result instead of a decline. One consequence of this error would be a poor production-profile prediction.

ITSPM. Once all four models are trained and verified, it is time to put them together into an integrated system that is capable of predicting the entire field's production. We are calling this integrated system a time-successive model because its prediction at each time depends on the previous-timestep predictions.

The time-successive model is tested on the same numerical-simulation model that was discussed before. At the beginning of 1987, the last set of production data for the 156 wells is obtained from the simulator. This data set is used to initialize the ITSPM. At each timestep, depending on the state of the well, one of the four designed models is used to predict its next-timestep production rate. At each timestep, the next production is predicted for all the wells. If at any time a new well is drilled using the initial-rate-prediction model, its initial rate is predicted and the well is added to the list of the producing wells. Because the first step systems' inputs are generated on the basis of the previous step's outputs, the model is completely independent from the simulation model's result.

It should be noted that COWs are determined dynamically, meaning that during the part of the reservoir's lifetime when new wells are added to the reservoir, each well's offsets are changing. In order to address this, offset wells for each well are recalculated at each timestep.

Implementing this step is performed in Visual Basic environment. A controller program is designed and tested. The program uses ".dll" files. These files are called inside the program at each timestep for each well, depending on which one fits the well's state of production.

Sensitivity Analysis

All pieces of information we have about any reservoir characteristics are subject to a high degree of uncertainty. Well-log informa-

tion is normally available only for a few percent of existing wells in the field. Moreover, this information is not an exact representation of geological characteristics and has an amount of uncertainty associated with it.

Also, the modeling part will have some uncertainty because of the errors associated with any predictive model. Therefore, the predicted values for production rate will not be exact. In order to account for all these uncertainties and make sense of their effect on our technique, a sensitivity analysis is performed. A triangular distribution is considered for all the input values with a support range equal to 40% of the total range for that parameter while the actual value is most likely the value of the distribution.

A Monte Carlo simulation is performed for each predictive model using these input value distributions. The model's output would also be represented with a triangular distribution from which a minimum, maximum, and most-likely value for the output can be found.

Results

Neural-Network Results. Initial-Production-Rate Model. This model, which is the most uncertain part of the prediction, is predicting the initial rate of the new wells. Previously, we discussed that this neural-network model is trained on the basis of existing-well instances during the reservoir's lifetime.

The training set contains 133 well records. The crossplot for predicted initial-rate values and the actual value of the flow rate is shown in Fig. 10.

Second- and Third-Month Production-Rate Model. After predicting the initial rate, the second- and third-month production rates are modeled by other neural networks that are trained in the same manner. 10% of the data is used for calibration, and another 10% is kept for verification of the second-month model. For the third month, 5% is used for calibration and 5% for verification. Results of these models are shown in Figs. 11 and 12. As can be observed, the uncertainty of the prediction has decreased because more information about the wells is available when predicting the second month of production.

It can be observed that the results of the second and third month of production have a similar degree of accuracy. But when compared to the initial-rate prediction we see a more significant difference in the R^2 indicator (correlation factor). This is obviously because once the initial rate is predicted, much more information about the well and its behavior is revealed to the network so the last two networks have a much easier task to perform compared to the initial-rate prediction, which mostly used the available information at offset locations.

Tail-of-Production Model. This model predicts the production-rate change at each time of the well's life after the third month of production. The model is trained, calibrated, and verified with

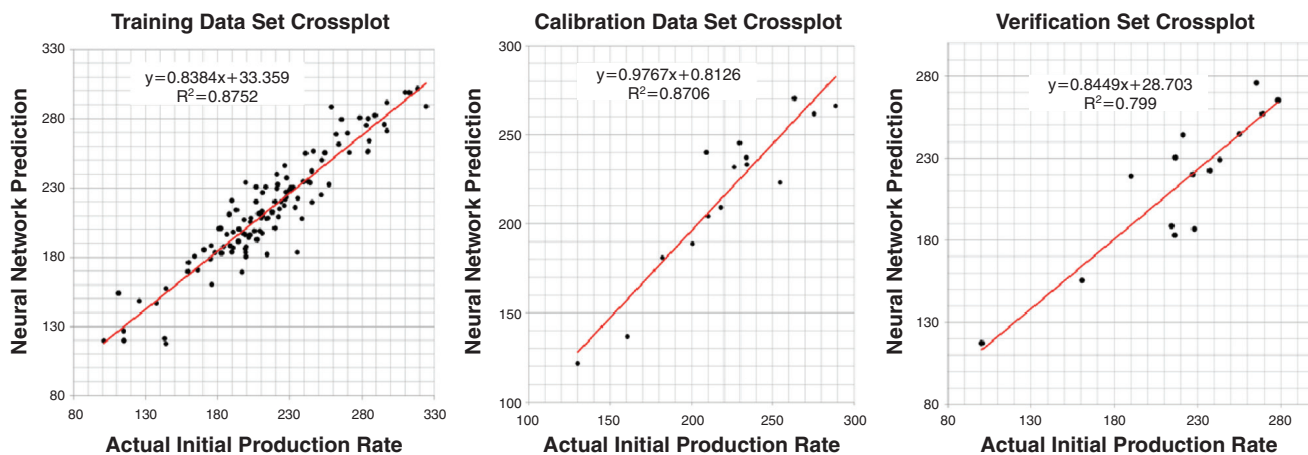


Fig. 10—Initial-rate-prediction neural-network-model results.

approximately 5,700 data records. Data are partitioned with a 60% training fraction, 20% calibration, and 20% verification part.

The training-, clarification-, and verification-data-set crossplots are shown in Fig. 13. These graphs show that the trained network also works very well for the blind data.

Time-Successive Model. The models that are represented in the neural-network results are used to build the integrated system for ITSPM. Production data were recorded from the simulation model from beginning of 1982, which was the first date of production of the first set of wells. Five years of this production data was used for training purposes, and another year was kept for verification.

The time-successive predictive model was initiated on 1 January 1987. A 1-year prediction of all the wells, including nine wells that were drilled after this date, is compared to the real production data from numerical-simulator results.

Predicting the production of a new well is the main objective of this work. The entire-field and all existing-well production is also predicted and can be compared to the conventional decline-curve-analysis results. The precision of these predictions will increase the validity of new-well-production prediction. Interestingly, this method let us predict the decline behavior of a well that has not been drilled yet. This will lead to better decision making and performance assessments.

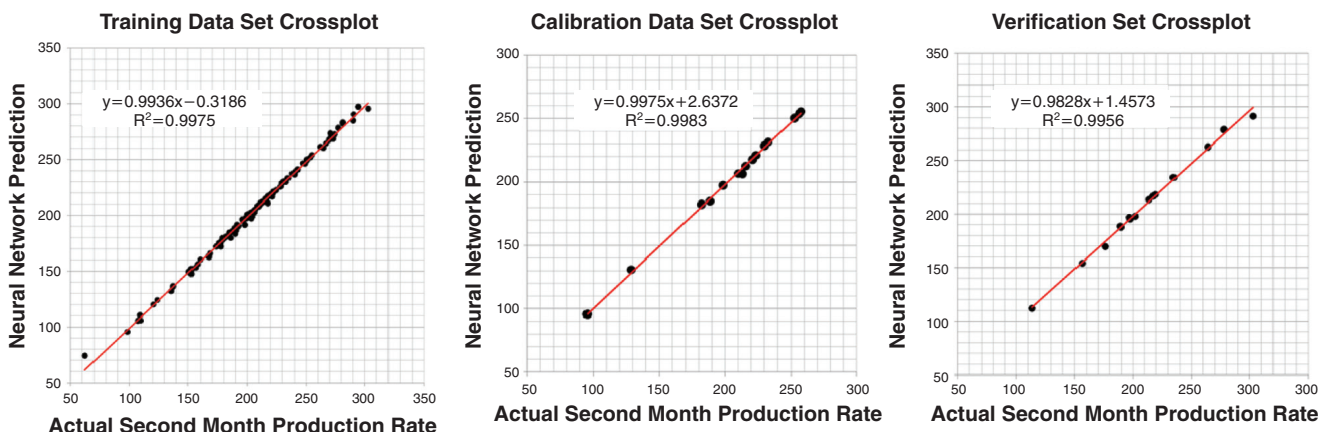


Fig. 11—Second-month production-rate-prediction neural-network-model results.

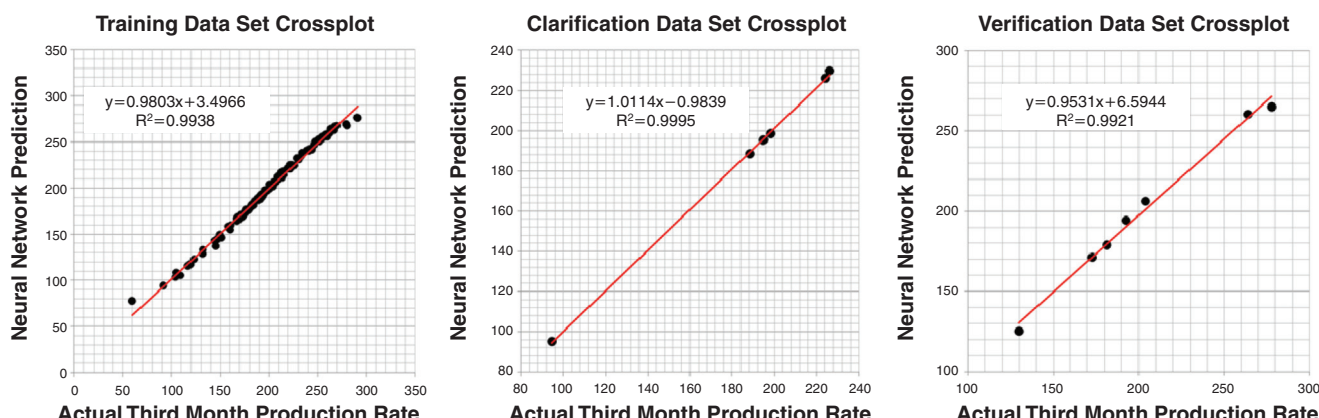


Fig. 12—Third-month production-rate-prediction neural-network-model results.

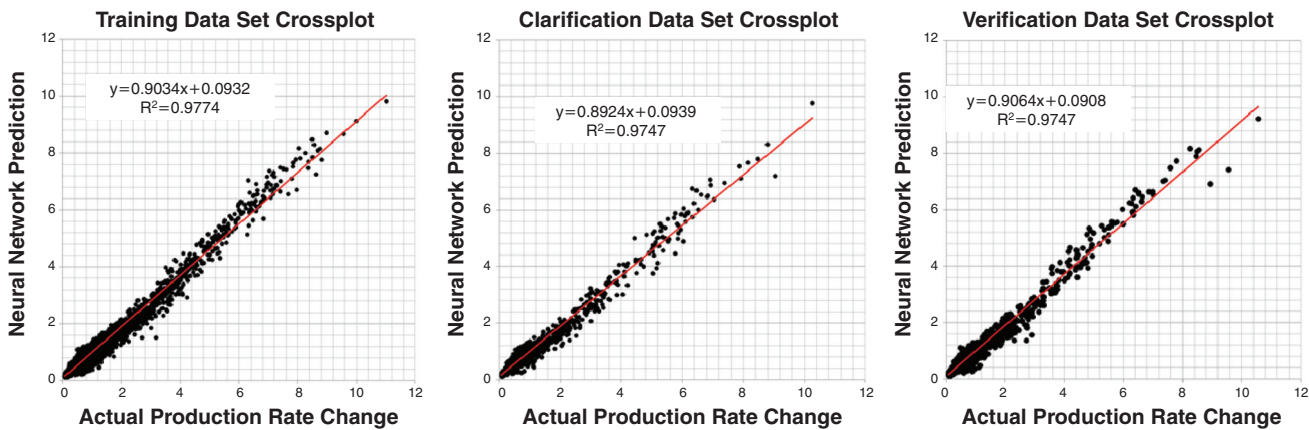


Fig. 13—Tail-of-production-prediction neural-network-model results.

Nine wells were kept out of all the trained models, and now their production is estimated through the time-successive prediction model. These flow predictions are compared with real results taken from the numerical simulator. Fig. 14 shows the nine new wells' flow-rate profile and cumulative-production comparison. In these figures, the actual production rates are shown in red and the production prediction is in blue. The purple curve shows the actual cumulative production, while the green curve shows the predicted cumulative production.

The total-field production prediction and one of the old well's production predictions are also compared to the actual value from the numerical-simulation results (Fig. 15).

Sensitivity Analysis. The results of the Monte Carlo simulation described before are presented for two of the new wells. These results can be compared with those from time-successive model.

As can be seen in Fig. 16, the most likely prediction stays very close to the real production profile despite the uncertainties involved with all the input parameters while the minimum and maximum range show the extent of possible output values from this technique.

Application of ITSPM to Two Real Giant Oil Fields

In order to examine the validity of this technique, its applicability to two real cases is studied. The two cases are both huge fields in

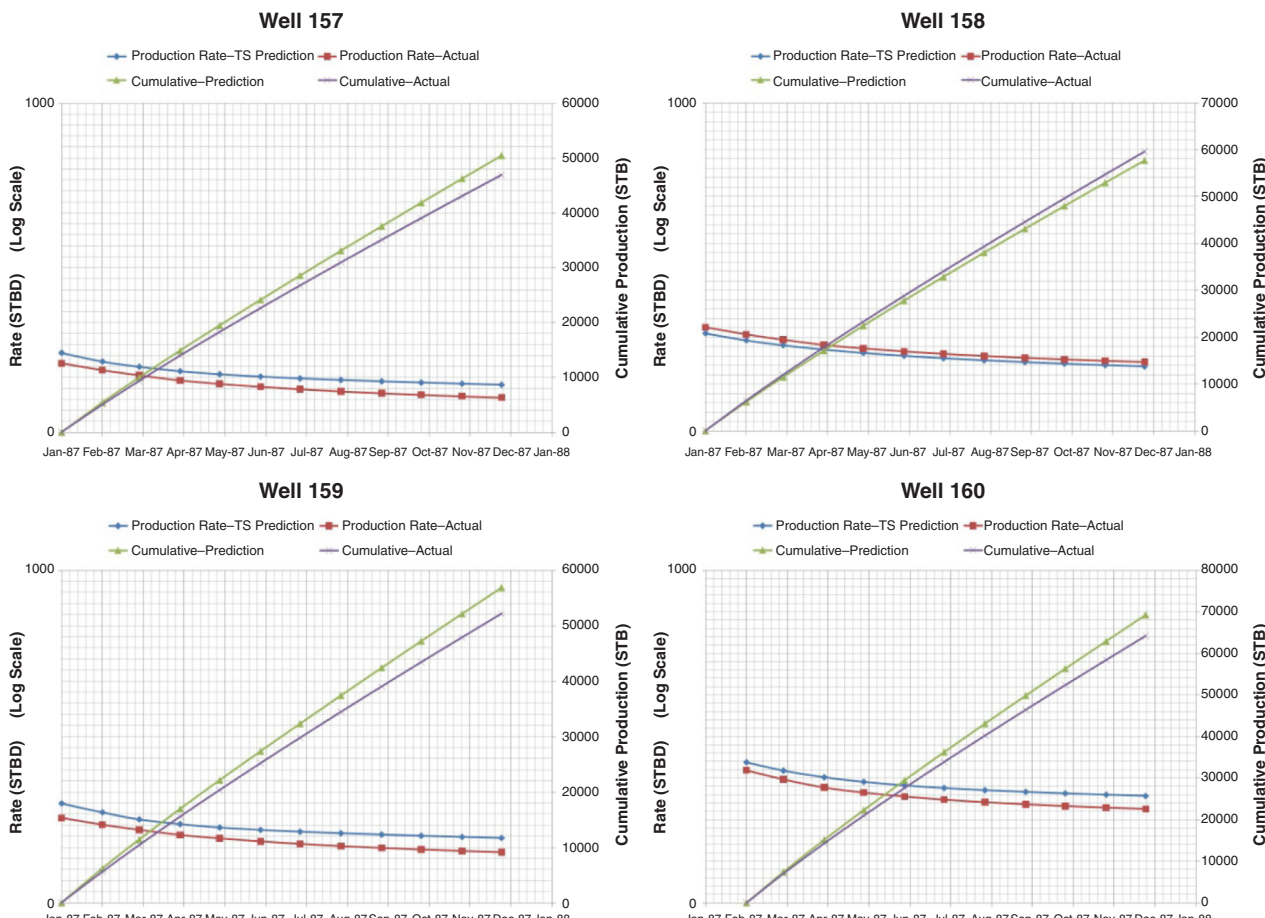


Fig. 14—Production prediction for nine new wells in the synthetic reservoir compared with the real production.

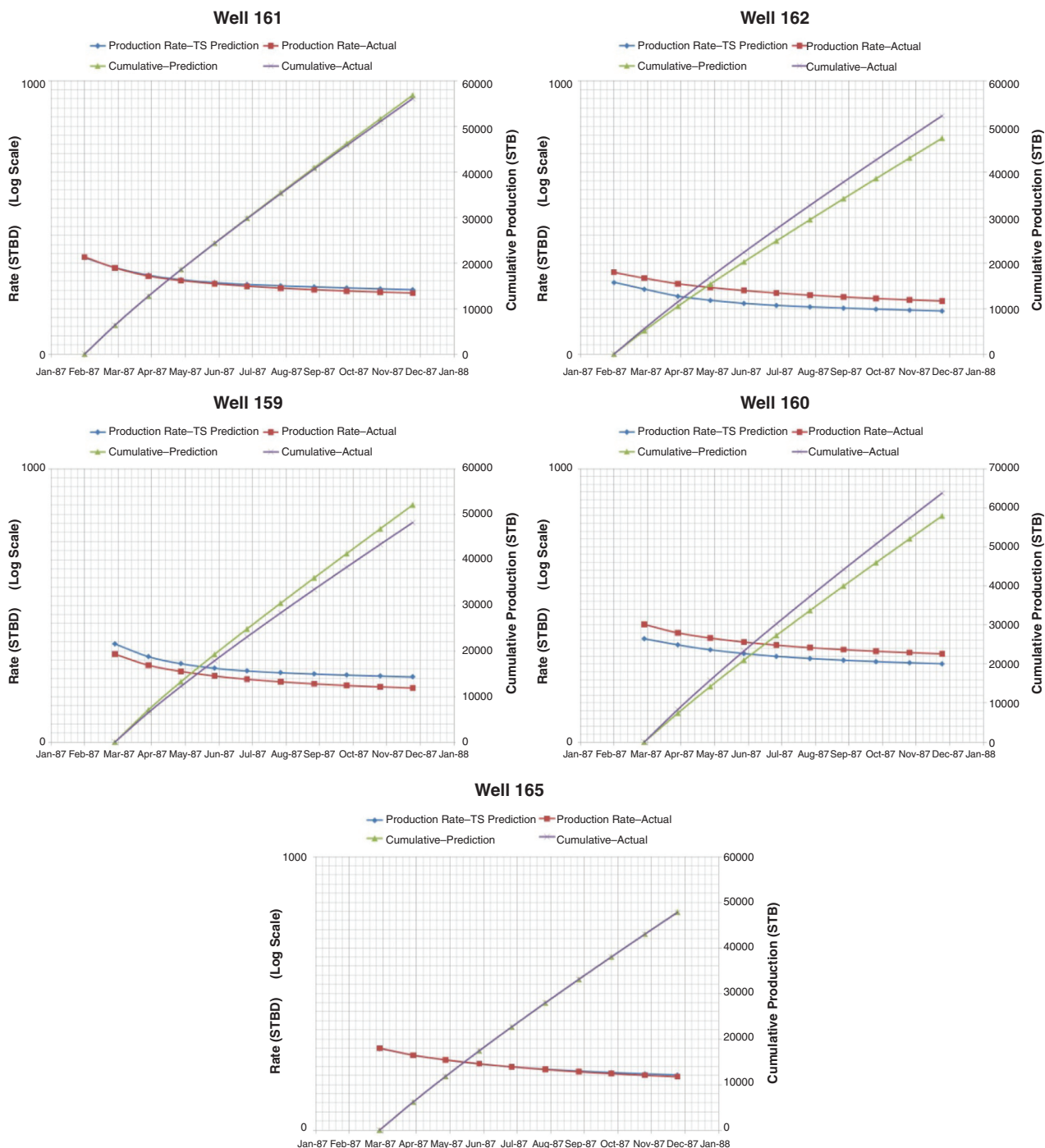


Fig. 14 (continued)—Production prediction for nine new wells in the synthetic reservoir compared with the real production.

the Middle East, with oil being the main production fluid. The first oilfield history contains more than 40 years of production data and reservoir characteristics at well locations.

This field has 210 oil-producing wells. The wells were drilled between 1963 and 2001. The wells' location and EUDA assigned to them by the Voronoi technique are shown in **Fig. 17**.

Available static information about this field includes porosity and formation net pay at the wells. Also, permeability value obtained from well tests and flowing bottomhole pressure are available. Initial pressure of the reservoir is 4,437 psi, and initial temperature is 190°F. Ranges for these parameters are shown in **Table 2**.

Production data contain noise and uncertainty. In order to reduce this noise before we use the data from the time-successive prediction method, decline-curve analysis is performed for each

well and the decline-curve data replace real production data. Out of 210 wells that are producing in the field, the four most recent wells, drilled in 2001, are taken out for verification purpose. The data set is built on the basis of geological information and oil-production data from 206 wells.

Data-set generation follows the same path described previously. The five COWs are located, and their information is included in the data set. Looking at the initial rate of production of the 206 existing wells, a declining trend during the life time of the reservoir is apparent. This can be explained by depletion of the reservoir over 40 years of production. Because of this decreasing trend, the initial rate of the new wells would be more correlated to the latest existing wells than to the older ones. To address this issue of depletion, the last 20 years of production data was used to model the initial rate of production.

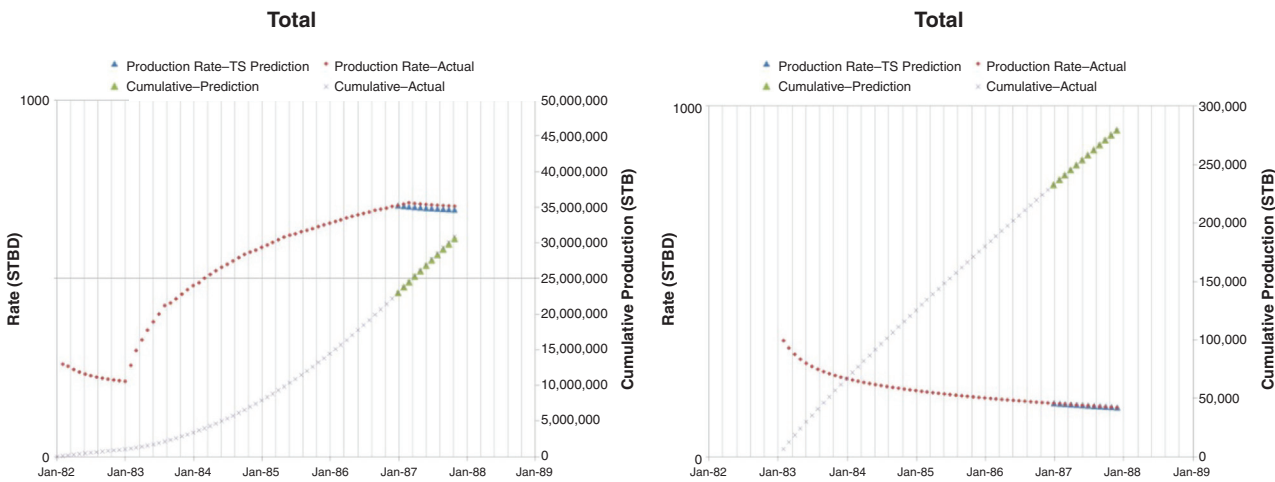


Fig. 15—Total-field production prediction compared to real data (left); one existing well's future production compared to real data (right).

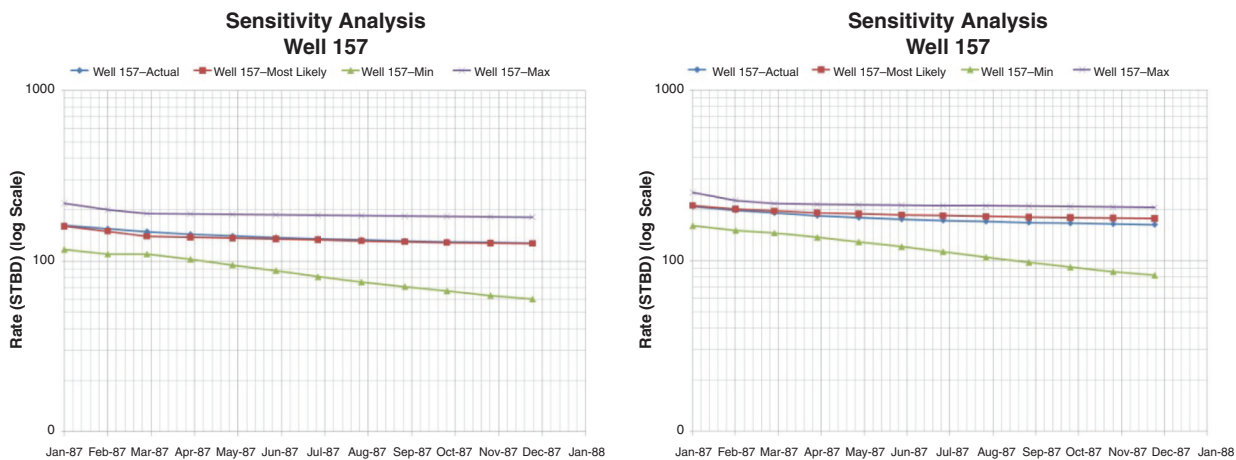


Fig. 16—Monte Carlo simulation results for two new wells.

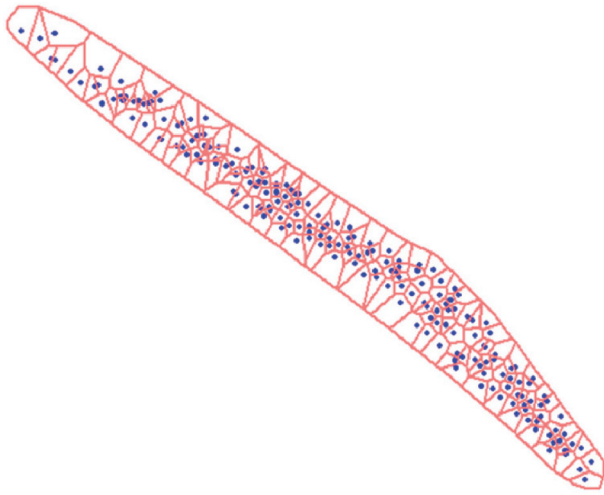


Fig. 17—Real-field wells and EUDA.

In the first model, a neural network is trained using the backpropagation technique. Selected inputs are shown in **Fig. 18**.

Results of this model are presented in **Fig. 19**. The real initial production rate is compared to the predicted value. As can be observed from the comparison graph, the initial-rate prediction is the most uncertain part of this modeling method. At some points, the prediction experiences a larger error, but more than 80% of the predictions experience less than 30% error.

For the second and third month of the production, two separate models are designed and two neural networks are trained and verified. Unlike the synthetic model, the output of neural networks is the cumulative production rather than the rate at each timestep. The cumulative production seemed to be a better choice for prediction because of its less-noisy behavior and always-increasing nature. In the second-month cumulative-production-prediction model, the preceding-month cumulative is used as an input, and the two-preceding-months data are used as inputs for the third month. Networks selected inputs are shown in **Fig. 20**. These inputs are selected on the basis of a key-performance-indicator analysis.

TABLE 2—REAL-FIELD GEOLOGICAL-PROPERTIES RANGES

Property	Porosity (%)	Net Thickness (ft)	Permeability (md)	Initial Oil Saturation	Flowing Bottomhole Pressure (psia)
Minimum	10.00	170.56	3.04	63.00	1500.00
Maximum	21.00	3462.37	4679.00	83.00	4079.00

Selected Input Parameters	
Well's	Closest Offset's
Formation Thickness	First Offset Initial Rate
Initial Oil Saturation	Second Offset Initial Rate
Location Lat and Long	Fourth Offset Initial Rate
Date of First Production	First Offset Time Difference in Date of first Production
	Second Offset Time Difference in Date of first Production
	Distance to First Offset Well
	Distance to Second Offset Well
	First Offset Well's Current Production Rate
	Second Offset Well's Current Production Rate

Fig. 18—Initial-production-rate-prediction model—input list.

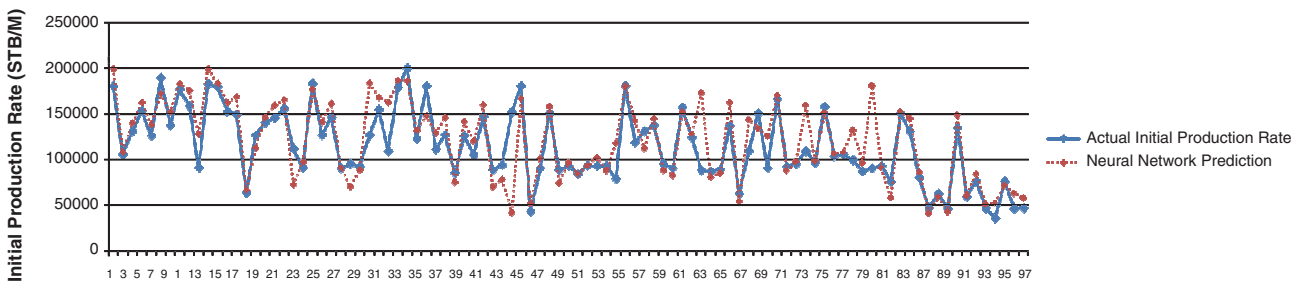


Fig. 19—Initial-production-rate prediction model, performance behavior (97 wells are used in this model).

Selected Input Parameters	
Well's	Closest Offset's
Formation Thickness	Fourth Offset Initial Rate
Initial Oil Saturation	Third Offset Initial Rate
Porosity	First Offset Time Difference in Date of first Production
Flowing Bottom-hole Pressure	Second Offset Time Difference in Date of first Production
Initial Production Rate	Third Offset Time Difference in Date of first Production
Date of First Production	Distance to First Offset Well
	Distance to Second Offset Well
	Distance to Third Offset Well
	First Offset Well's Current Production Rate
	Second Offset Well's Current Production Rate
	Third Offset Well's Current Production Rate

Selected Input Parameters	
Well's	Closest Offset's
Initial Oil Saturation	Fourth Offset Initial Rate
	First Offset Time Difference in Date of first Production
Initial Production Rate	Second Offset Time Difference in Date of first Production
Second Month Production Rate	Date of First Production
	Distance to First Offset Well
	Second Offset Well's Current Production Rate
	Fifth Offset Well Estimated Ultimate Drainage Area

Selected Input Parameters	
Well's	Closest Offset's
Porosity	First Offset Well's Porosity
Initial Oil Saturation	Second Offset Well's Porosity
Formation Thickness	Fourth Offset Initial Decline Rate
Permeability (Well Test Results)	
Well's Location Lat and Long	
Initial Oil Saturation	
Initial Production Rate	
Three preceding Months' Cumulative Production	
Date of First Production	

Fig. 20—Second-month cumulative-production-prediction model, input list (left); third-month cumulative-production-prediction model, input list (center); cumulative-production-prediction model, input list (right).

Results of the last three models—second- and third-month production along with the cumulative production of the well during the time—are also shown in Figs. 21 through 23, respectively.

In the first of these models (Fig. 21), more than 80% of the predictions have less than 5% error.

In the second model (Fig. 22), more than 90% of the predictions have less than 5% error.

In the third model (Fig. 23), more than 80% of the predictions have less than 5% error.

Now that all the models are trained and verified, they can be used to predict the future production of four new wells. These wells described have not been used in any of the data sets and none of their characteristics have been available to the networks. These four well locations are shown in Fig. 24.

Production predicted for these four wells is compared with the reality. Results are shown in Fig. 25.

As can be seen in Fig. 25, visible in three out of four wells, a fairly good prediction of cumulative production is obtained.

Real-Field Case With Waterflooding. In the second attempt, the ITSPM method is applied to an oil field that has multiple active productive layers. The field has been under edgewater injection for most of its life. Some time-lapse water-saturation data are available for a few wells. Each well has been logged at the spud date, so porosity and initial-water-saturation data are available. Also an indication of the permeability value is available, based on initial well logs. Oil- and gas-production data are recorded separately for each producing layer by allocating the total production on the basis of the thickness and permeability of the layers.

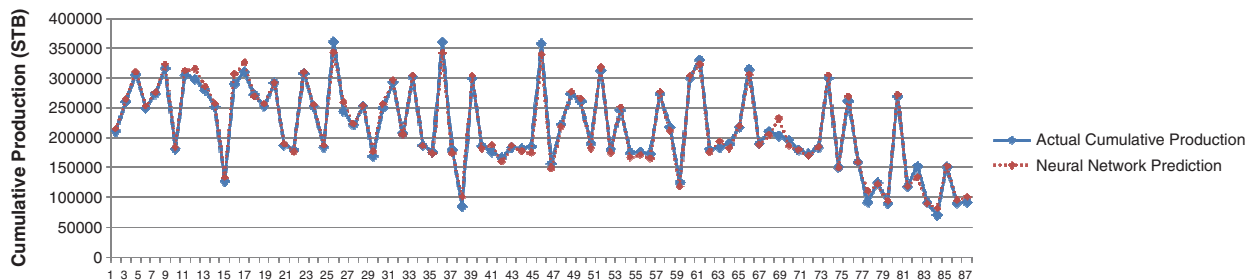


Fig. 21—Second-month cumulative-production-prediction model, performance behavior (87 wells are used in this model).

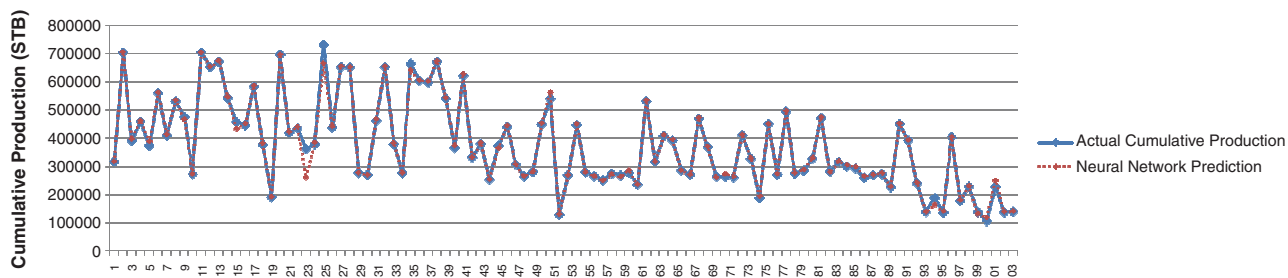


Fig. 22—Third-month cumulative-production-prediction model, performance behavior (103 wells are used in this model).

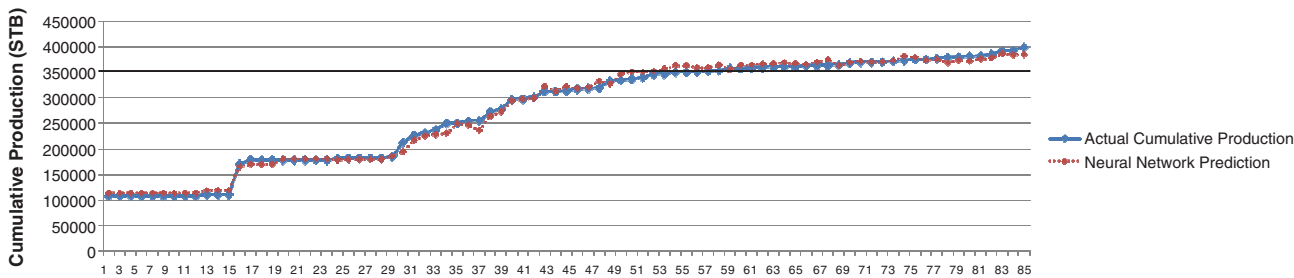


Fig. 23—Cumulative-production-prediction model, performance behavior (85 wells are used in this model).

Because we are in the process of securing agreement of publication for this work, only a sample of the results are shown in this paper. The complete study with details will be published in a future paper. For the same reason, no maps can be shown from the field and the scale of the production is removed in the graphs, but they can still be used to validate the results of ITSPM prediction against the real production data.

Data Preparation for the Real Field. In this field, an initial log is available for most of the production and some of the injection wells. These logs provide porosity, permeability, and initial water saturation for the wells. For each reservoir characteristic (porosity, permeability, and initial water saturation), a distribution map is built using the well-log values. These maps are used throughout the study, and as more data become available, the map is updated.

Time-lapse water-saturation data are also available at some wells. These values are incorporated to generate water-saturation distribution as a function of time.

All these different pieces of information are used to build the data set for this reservoir. Each well's characteristics and production history, along with the time-lapse water-saturation information, make the data record for that well. On the other hand, information from three production offset wells and two injection offset wells is included in each well's record. This knowledge base is used to build predictive models that can forecast the well's future production as well as any infill well's future production in the same manner that was presented in the preceding sections.

The reservoir has multiple production layers, and each reservoir layer includes an average of 70 completed wells. Some wells are producing from more than one unit. Each productive unit needs a separate predictive model. The first 30 years of production history is used for building the predictive model. The rest of the production data until present time is used for validation of the models.

Predictive Models. In this case study, in addition to the well's production, we had access to some water-saturation values as a function of time. This resulted in a design for the system that included

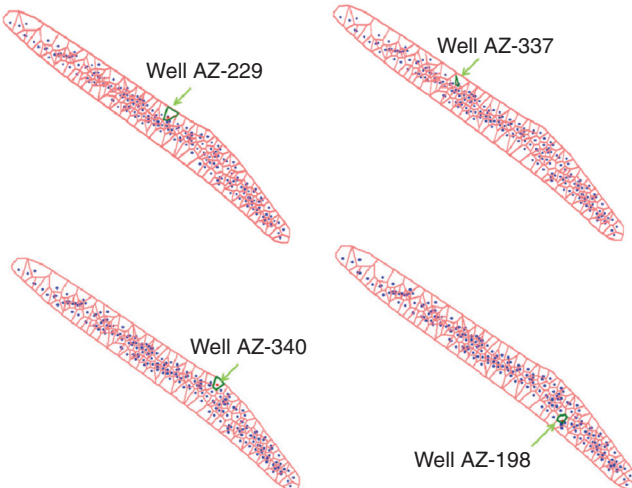


Fig. 24—Four verification-well locations.

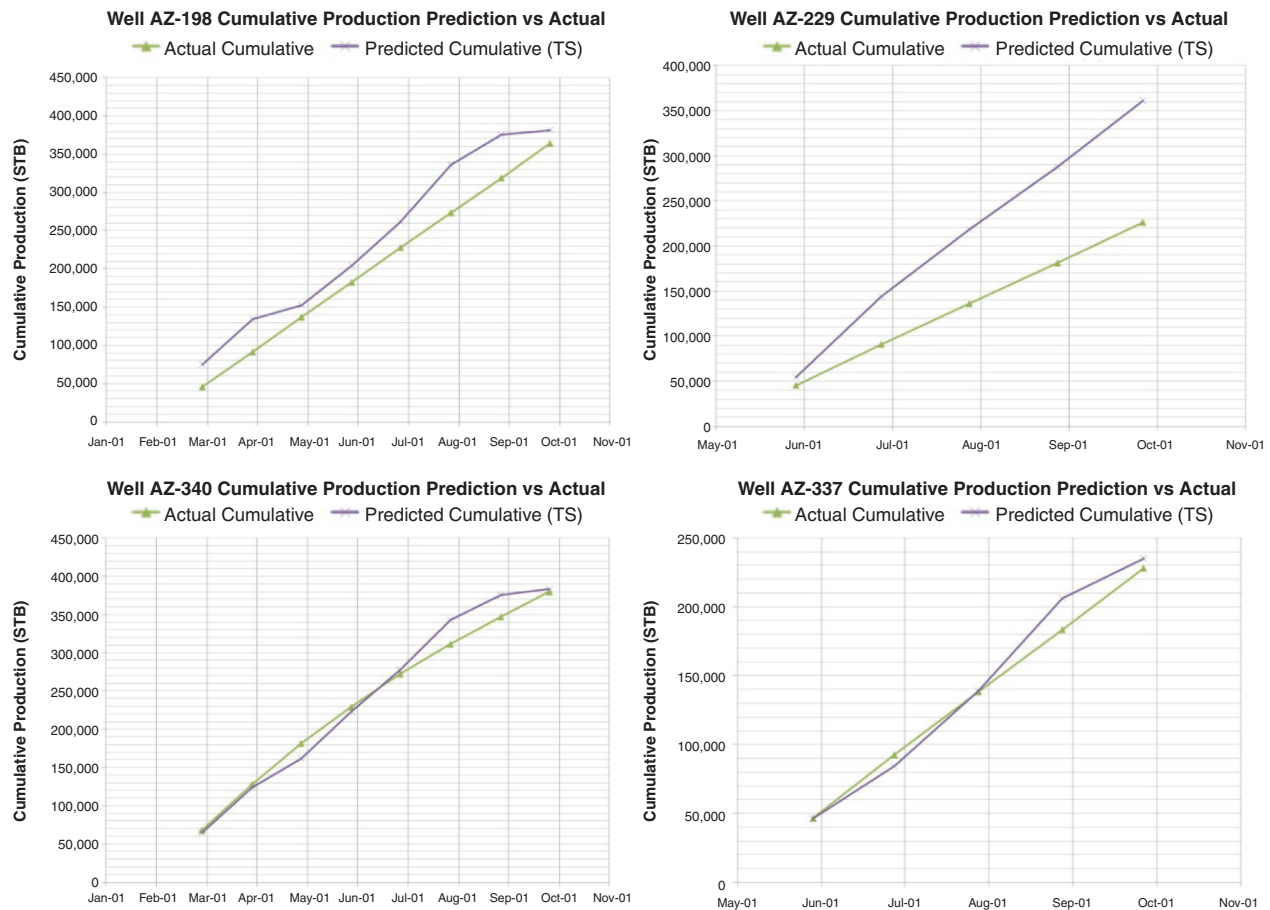


Fig. 25—Production prediction of four new wells in the real field.

the use of time-lapse water-saturation values as part of the input to the predictive model for the production rate. To accommodate this new design a separate model for the time-lapse water saturation was developed. Therefore, the final predictive model for this study included multiple interacting models (time-lapse water-saturation and production-rate models). Furthermore, data representing the operational constraints were included in all the models.

Water-Saturation Model. The predictive model for water saturation provides a water-saturation value at each well location at any given time. These values are then used in the next model to

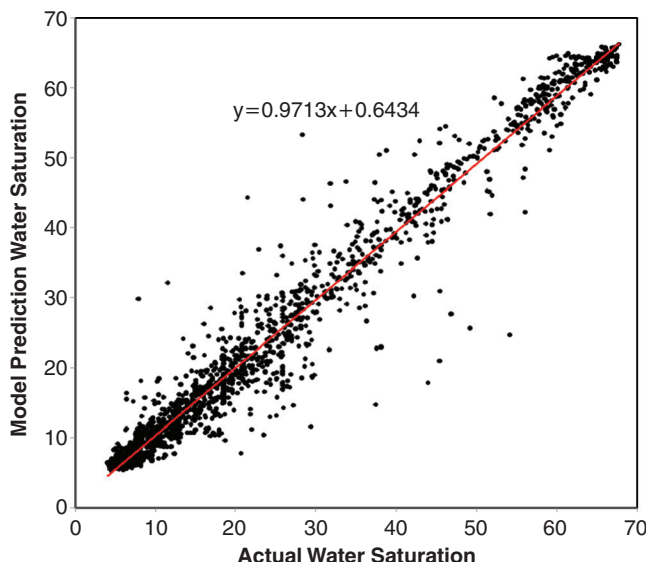


Fig. 26—Water-saturation predictive-model results.

predict the amount of oil production. Results of this model are shown for one of the productive layers in Fig. 26. The crossplot shows the predictions from the model's output vs. the actual values (field measurements). The model is a multilayer neural network that is trained using a back-propagation technique. Each point in the graph represents a water-saturation value at one of the wells at a given time during that well's life.

Oil-Production Model. The next predictive model is aimed at predicting the oil production for each well during time. This model uses the complete data set and includes the results from the water-saturation model. The model is based on a multilayer neural network, trained by a back-propagation technique. In order to evaluate the validity of the model, a crossplot of its output vs. the actual production data from the field is shown in Fig. 27.

Each productive layer has a separate model for water saturation and oil production. These models that are developed separately can be combined to predict the complete production profile of the field. In Figs. 28 through 30, the prediction results for some of the wells in different productive layers are shown.

The highlighted parts of the graphs show the region where ITSPM has made predictions without using any data from that time frame (blind history match). Please note that actual production values (y-axis) have been removed because of confidentiality issues.

Conclusions and Discussions

This work was dedicated to a formal presentation of the concept of a spatio-temporal-data-driven modeling technique and its applicability to production-data analysis. In this study, we presented a new workflow for production prediction. It shows that incorporating the spatio-temporal dependencies of fluid flow in the porous media and its footprints in production data enables us to build a fieldwide model from multiple, individual single-well models. These spatial and temporal dependencies are addressed by incorporating the information content of the COWs in the model.

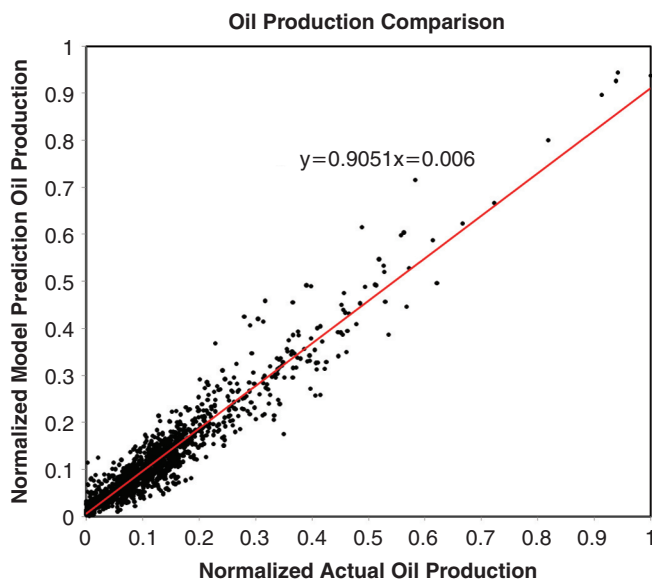


Fig. 27—Oil-production predictive-model results.

Geostatistic methods provide a full-field perception of the geological characteristics used in developing the fieldwide model. In this approach, the fieldwide comprehension of the reservoir behavior is accomplished with a single-well production-data analysis.

The Voronoi delineation of the reservoir gives a spatial definition of the single-wells analysis. By estimating the ultimate drainage area, the original hydrocarbons in place for each well is also predictable. Even though this may not project the exact amount of reserves surrounding each well, it provides a relative understanding of a well's future performance.

The limitation of this technique is its dependency on data availability. This will be an issue in cases with few wells and a low amount of past production. However, older brownfields will make good candidates for this technique.

ITSPM was applied successfully to a synthetic reservoir and two real fields. These cases all confirm the applicability and validity of this method. The diversity of the cases (one synthetic single phase, two real cases with multiphase flow, including one with waterflooding) shows that the method is not limited to simple problems. The ability of the method to handle different types of wells, dynamic completions during the time, shut-in periods, and infill drilling is also verified (during the second case study). ITSPM can be a promising technique, especially in cases with a long history of production data. The more data available for any field, the higher the possibility of success for this method. The key to any data-driven model is the amount and accuracy of the data. Nevertheless, one more important point is how to get the most out of this available information. We believe that ITSPM is able to bring out the hidden information about the reservoir characteristics and its behavior, which is embedded within the production and field data. This technology has been incorporated in the top-down, intelligent-reservoir-modeling workflow that has been referenced extensively in this manuscript (Mohaghegh et al. 2005; Mohaghegh 2009; Gomez et al. 2009; Mohaghegh et al. 2011).

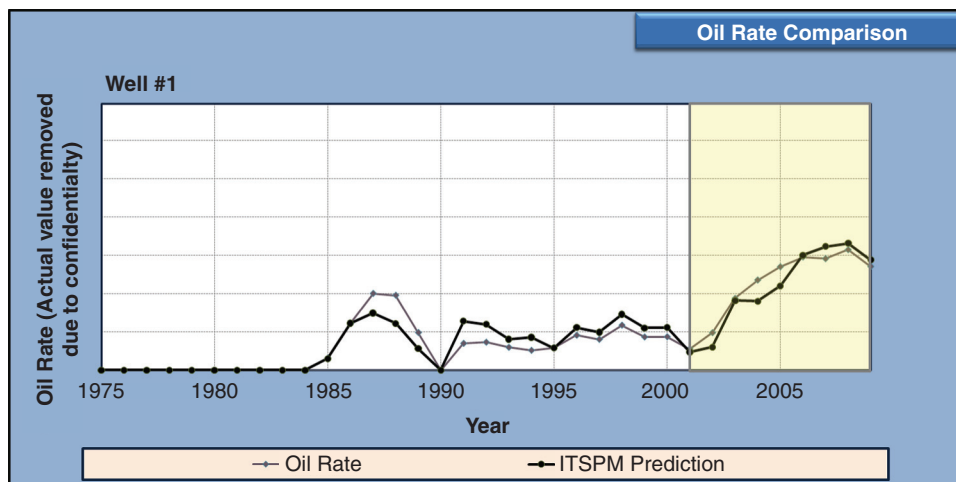


Fig. 28—Well No. 1 oil-production prediction from ITSPM compared to actual values.

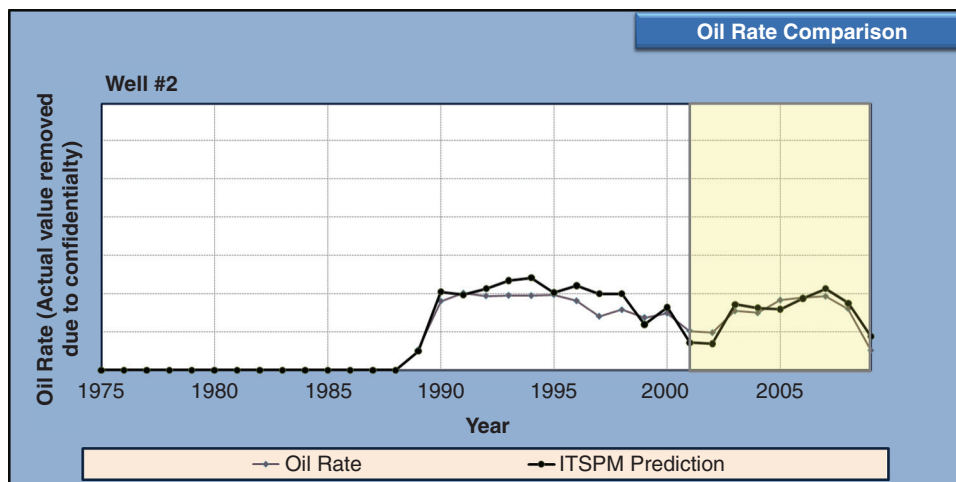


Fig. 29—Well No. 2 oil-production prediction from ITSPM compared to actual values.

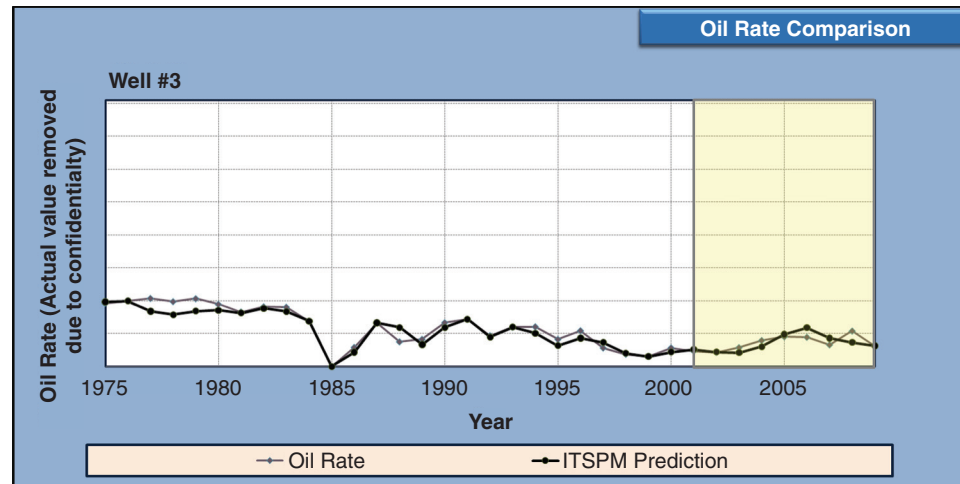


Fig. 30—Well No. 3 oil-production prediction from ITSPM compared to actual values.

Acknowledgments

The authors of this paper would like to thank the Computer Modeling Group Limited for providing the academic license for the CMG/IMEX reservoir simulator for performing the numerical modeling of the synthetic case study. We also thank and acknowledge Intelligent Solutions for providing IDEA software to perform the neural-network modeling (for the synthetic and the two real-field case studies). Also, the authors would like to acknowledge the members of the Petroleum Engineering and Analytics Research Laboratory at West Virginia University for their assistance and support.

References

- Agarwal, R.G., Gardner, D.C., Kleinsteiber, S.W., and Fussell, D.D. 1999. Analyzing Well Production Data Using Combined-Type-Curve and Decline-Curve Analysis Concepts. *SPE Res Eval & Eng* 2 (5): 478–486. SPE-57916-PA. <http://dx.doi.org/10.2118/57916-PA>.
- Arps, J.J. 1945. Analysis of Decline Curves. In *Petroleum Development and Technology 1945*, Vol. 160, SPE-945228-G, 228–247. New York: Transactions of the American Institute of Mining and Metallurgical Engineers, AIME.
- Carter, R.D. 1981. Characteristic Behavior of Finite Radial and Linear Gas Flow Systems—Constant Terminal Pressure Case. Paper SPE 9887 presented at the SPE/DOE Low Permeability Gas Reservoirs Symposium, Denver, 27–29 May. <http://dx.doi.org/10.2118/9887-MS>.
- Chauvin, Y. and Rumelhart, D.E. ed. 1995. *Backpropagation: Theory, Architectures, and Applications*. London: Psychology Press/Taylor & Francis Group.
- Fanchi, J.R. 2005. *Principles of Applied Reservoir Simulation*, third edition. Oxford, UK: Elsevier.
- Fetkovich, M.J. 1980. Decline Curve Analysis Using Type Curves. *J Pet Technol* 32 (6): 1065–1077. SPE 4629-PA. <http://dx.doi.org/10.2118/4629-PA>.
- Gomez, Y., Khazaeni, Y., Mohaghegh, S.D., and Gaskari, R. 2009. Top Down Intelligent Reservoir Modeling. Paper SPE 124204 presented at the SPE Annual Technical Conference and Exhibition, New Orleans, 4–7 October. <http://dx.doi.org/10.2118/124204-MS>.
- Haykin, S. 1999. *Neural Networks, a Comprehensive Foundation*, second edition. Upper Saddle River, New Jersey: Prentice-Hall Inc.
- Maren, A.J., Harston, C.T., and Pap, R.M. 1990. *Handbook of neural computing applications*. San Diego, California: Academic Press.
- Mohaghegh, S.D. 2000. Virtual-Intelligence Applications in Petroleum Engineering: Part 1—Neural Networks. *J Pet Technol* 52 (9): 64–73. SPE-58046-MS. <http://dx.doi.org/10.2118/58046-MS>.
- Mohaghegh, S.D. 2009. Top-Down Intelligent Reservoir Modeling (TDIRM): A New Approach in Reservoir Modeling by Integrating Classic Reservoir Engineering with Artificial Intelligence & Data Mining Techniques. Paper presented at the 2009 AAPG Annual Convention, Denver, 7–10 June.
- Mohaghegh, S.D., Gaskari, R., and Jalali, J. 2005. A New Method for Production Data Analysis To Identify New Opportunities in Mature Fields: Methodology and Application. Paper presented at the SPE Eastern Regional Meeting, Morgantown, Morgantown, West Virginia, USA, 14–16 September. <http://dx.doi.org/10.2118/98010-MS>.
- Mohaghegh, S.D., Grujic, O.S., Zargari, S., and Dahaghi, A.K. 2011. Modeling, History Matching, Forecasting and Analysis of Shale Reservoirs performance Using Artificial Intelligence. Paper SPE 143875 presented at the SPE Digital Energy Conference and Exhibition, The Woodlands, Texas, USA, 19–21 April. <http://dx.doi.org/10.2118/143875-MS>.
- Okabe, A., Boots, B., Sugihara, K., and Chiu, S.N. 2000. *Spatial Tessellations: Concepts and Applications of Voronoi Diagrams*, second edition. West Sussex, UK: Wiley Series in Probability and Statistics, John Wiley & Sons.
- Palacio, J.C. and Blasingame, T.A. 1993. Decline-Curve Analysis Using Type Curves—Analysis of Gas Well Production Data. Paper Oral presentation presented at the Rocky Mountain Regional/Low Permeability Reservoirs Symposium and Exhibition, Denver, 26–28 April. <http://dx.doi.org/10.2118/25909-MS>.
- Yasaman Khazaeni** is a PhD student in Systems Engineering at Boston University. Previously, Khazaeni was a research scientist in the petroleum and natural gas engineering department at West Virginia University for more than a year after finishing her Masters studies in the same department. With more than 5 years of experience in petroleum and natural gas engineering, she has worked on several research projects related to application of artificial intelligence and data mining in this industry. She has published several technical papers and has presented in SPE international conferences and also served as a discussion leader in SPE Forums. She holds two BS degrees in electrical engineering and petroleum engineering from Sharif University of Technology in Iran and an MS in petroleum and natural gas engineering from West Virginia University. **Shahab D. Mohaghegh** is a professor of petroleum and natural gas engineering at West Virginia University. Mohaghegh has been a pioneer in the application of intelligent systems in petroleum engineering. Mohaghegh holds BS and MS degrees in natural gas engineering from Texas A&M University and PhD in petroleum and natural gas engineering from The Pennsylvania State University. He has published more than 50 technical papers during his career and has been a technical editor/reviewer for various SPE journals as well as other petroleum-related publications such as Journal of Petroleum Science and Engineering, Computers & Geosciences, Geophysics, and Energy & Fuels. He was the technical review chair for SPE Reservoir Evaluation and Engineering Journal from 1997–99, where he currently serves as a technical editor. He has also served as discussion leader and technical presenter in SPE forums and has served as a steering committee member in SPE Applied Technical Workshops.